Brain Research, 599 (1992) 283–296

BRES 18382

The effects of selective glutamate receptor antagonists on synchronized firing bursts in layer III of rat visual cortex

Ronald B. Langdon and Mriganka Sur

Department of Brain and Cognitive Science, Massachusetts Institute of Technology, Cambridge, MA 02139 (USA)

(Accepted 28 July 1992)

Key words: α-Amino-3-hydroxy-5-methyl-4-isoxazolepropionic acid/kainate; *N*-Methyl-D-aspartic acid receptor; D-2-Amino-5-phosphonovalerate; 6-Cyano-7-nitroquinoxaline-2,3-dione

In the rat visual cortex in vitro, single-shock stimulations applied to the border between layer VI and the white matter evoke synchronized burst-firing by units in layer III. We have examined the effects of glutamate receptor antagonists on this activity, with antagonists applied via the bath to allow correlation of effects with concentrations. All synaptically driven components (recorded extracellularly as field potential 'S2' spikes, dipoles 'W1' and 'W2,' and coinciding single-unit spikes) were inhibited by greater than 90% in 1.0 mM kynurenic acid and in 3 or 10 μM 6-cyano-7-nitroquinoxaline-2,3-dione (CNQX, which selectively blocks AMPA/kainate receptors). S2 spike amplitudes were reduced by half in 0.7 μM CNQX. 2-Amino-5-phosphonovalerate (APV), a specific blocker of NMDA receptors, did not prevent S2 spike bursts or horizontal spread of bursting within layer III. However, APV reduced the duration of synchronized bursts and the slower potentials which followed. In Mg^{2+}-free medium, new components appeared which were APV-sensitive: (1) low amplitude spikes, distributed spatially like S2 spikes, but recurring more slowly, and (2) slow potentials, distributed spatially like W1 and W2 potentials, but lasting for hundreds of milliseconds. The amplitudes of these spikes were reduced by half in 3 μM D-APV. Our data imply that: (1) glutamate receptors play a major role in mediating local, excitatory neurotransmission in the supragranular layers of neocortex, with NMDA and AMPA/kainate subtypes each subserving somewhat different functions; (2) AMPA/kainate receptors mediate rapid excitatory transmission between layer III neurons, responsible for driving the first 15 ms of synchronized bursts; (3) currents gated by NMDA receptors determine the duration of coherent firing bursts, and drive asynchronous neuronal firing following bursts; and (4) under conditions which circumvent block by extracellular Mg^{2+}, activation of NMDA receptors greatly enhances and prolongs the response to single-shock stimulations. In vivo, activation of layer III neurons is likely to depend significantly upon currents gated by NMDA receptors whenever repetitively firing excitatory inputs summed over several tens of milliseconds provide enough depolarization to lift block by extracellular Mg^{2+}.

INTRODUCTION

A single-shock stimulation applied to the white matter evokes a brief burst of phase-locked firing by layer III units in slices of rat visual cortex maintained in vitro. Conjointly, this activity generates a brief field potential population spike burst[40]. The amplitude and spatial distribution of these bursts imply that they are generated by synchronously firing units concentrated within a narrow stratum of the neocortex. These phase-locked bursts require synaptic transmission and are most likely due to excitatory transmission between pyramidal cells in layer III, neurons which project both locally and to distant regions of neocortex[21,30,56,58]. In this present study, we examine the pharmacology of excitatory connections that drive synchronous firing in layer III in vitro.

Previously we found that glutamatergic neurotransmission is essential for all post-synaptic activity detected by our extracellular recordings[40]. Our main effort thereafter focused on resolving the respective contributions made by either of two different kinds of ionotropic glutamate receptor. These are: (1) NMDA receptors, which are particularly sensitive to the agonist *N*-methyl-D-aspartic acid and are blocked specifically by 2-amino-5-phosphonovalerate (APV); and (2) AMPA/kainate receptors, which are most effectively activated by kainate, quisqualate, or α-amino-3-hydroxy-5-methyl-4-isoxazolepropionic acid (AMPA) and blocked specifically by low micromolar concentrations

Correspondence: R.B. Langdon. Present address: Department of Behavioral Neuroscience, University of Pittsburgh, 446 Crawford Hall, Pittsburgh, PA 15260, USA. Fax: (1) (412) 613-9198.

of 6-cyano-7-nitroquinoxaline-2,3-dione (CNQX).

NMDA and AMPA/kainate receptors differ markedly in many respects besides their sensitivities to agonists and antagonists, and they clearly differ in their functions in the brain[10,13,19,24,28,36,60,64,68]. Whereas many synapses clearly use AMPA/kainate receptors to mediate rapid and brief excitatory neurotransmission, the function of NMDA receptors has been more difficult to discern and to define. Interest stems, in part, from the role of NMDA receptors in regulating synaptic plasticity in different regions of the brain, including the visual system (reviewed in ref. 12; see also refs. 4 and 25). However, the NMDA receptor channel has biophysical properties that could allow it to play distinctly different physiological roles than its counterpart, the AMPA/kainate receptor. The kinetics of receptor activation are significantly slower for NMDA receptors[5,34,44,50]. Moreover, the conductance of its ion channel normally depends upon the post-synaptic membrane potential. The activated channel is partially blocked by Mg^{2+} unless there is a sufficient summation of depolarization in response to excitatory inputs at the same synapse or at other synapses on the same cell. Consistent with this, it is the sustained responses to visual stimulation of neurons in the cat lateral geniculate nucleus (LGN) that are particularly dependent on NMDA receptors[28,36,64], as is the late component of excitatory post-synaptic potentials (EPSPs) evoked in LGN cells in vitro by stimulation of the optic tract[16]. In the visual cortex in vitro, responses of layer II/III neurons to ascending afferents are mediated by both AMPA/kainate and NMDA receptors, with NMDA receptors responsible for only the longer latency (and probably polysynaptic) single-unit spikes and the slower components of the intracellularly recorded EPSP[51]. In contrast, the visually driven response of some layer II/III cells in vivo appear to depend entirely upon activation of NMDA receptors[19,51].

In order to drive coherent firing of layer III pyramidal cells, transmission between cells must be effective within 3–5 ms[40]. Consistent with the evidence above on the role of NMDA and AMPA/kainate receptors in mediating excitatory neurotransmission, one might expect that this driving is mediated primarily by AMPA/kainate receptors. To test this hypothesis, we have applied APV and CNQX at concentrations at which they are believed to act specifically upon NMDA and AMPA/kainate receptors, respectively, while recording (1) field potential population spikes generated by synchronous firing bursts and (2) the activity of single units that fire in phase with these population spikes. To observe the full extent to which NMDA receptors may contribute to responses, we have examined the effects of these specific antagonists both in medium containing a normal level of Mg^{2+}, and in medium without Mg^{2+}. Our data demonstrate that AMPA/kainate receptors alone are responsible for driving the earliest spikes in each evoked burst, but activity of NMDA receptors can greatly prolong the duration of responses.

Some of these data have appeared previously in preliminary form[38,39,41].

MATERIALS AND METHODS

Laminar distributions of local field potentials were determined by methods which we have previously described in detail[40]. Briefly, our 'normal' slice medium was a solution composed of (in mM): NaCl 114; KCl 3; $CaCl_2$ 2.4, $MgCl_2$ 1.2; Na_2SO_4 1.2; D-glucose 10; glycine 0.001; HEPES 10; Phenol red 0.01; $NaHCO_2$ 25; sodium phosphate buffer (pH 7.0) 1; and sufficient (~ 2.5 mM) HCl to bring the pH to 7.3–7.4 when bubbled with 95% O_2 /5% CO_2. We refer to solutions to which we added no Mg^{2+} as 'Mg^{2+}-free'. To make Mg^{2+}-free medium, $CaCl_2$ was substituted for $MgCl_2$ (increasing the $[Ca^{2+}]$ to 3.7 mM).

To prepare slices of primary visual cortex ("Oc1" in refs. 71 and 72), albino rats (Charles River, 250–400 gm), were deeply anesthetized by intramuscular injection of ketamine HCl (100 mg/kg) and acepromazine maleate (10 mg/kg). The occipital half of the left cortical hemisphere was exposed. Following sacrifice (exsanguination by cardiac puncture), a block of brain that included the primary visual cortex was transferred to cold (4–8°C) slice medium in which 500 μm-thick coronal sections were prepared. All data were recorded from neocortex between 2.7 and 3.4 mm anterior to the interaural line[57]. Ketamine anesthesia is reported to reduce neurotoxic effects of anoxia during slice preparation[59]. Ketamine is an NMDA receptor antagonist, and would therefore interfere with our pharmacological study if it could not be washed out of the slices. However, antagonism of NMDA receptors by ketamine is readily reversed by application of drug-free medium to in vitro brain preparations[20,48]. Because reversal of channel block requires channel activation, our slices were subjected to hundreds of stimulations before data were recorded. All data were recorded at least 3 h after slice preparation, with the slices maintained completely submerged in moving medium throughout (see below), and stimuli delivered continuously at 25 per min. Under such conditions, it is highly unlikely that a significant level of NMDA receptor block remained.

We used a submersion-type slice chamber, with slices surrounded above and below by moving medium (maintained at 33°C) driven by a jet of O_2 /CO_2. Besides improving viability, this movement probably accelerated equilibration of drug concentrations during solution changes. Based on the field potential data, each slice was viable through its entire thickness and there was no apparent deterioration of responses throughout the 6–12 h over which data were collected[40]. When a drug or divalent ion concentration in the medium was changed, 15–20 min were required for complete equilibration of the responses to a new level. Therefore, all observations relating drug effects and drug concentration were made at least 20 min after changing the medium.

Each recording position was defined by using the intersection of the pial surface and the radial axis which intersected the site of stimulation as a point of reference, with the electrode mounted on a micropositioner with calibrated movement in the 3 orthogonal dimensions. We refer to displacement orthogonal to the pial surface as 'radial' and displacement parallel to the pial surface as 'horizontal.' 'Depth' refers to distance from the pial surface. A 'depth profile' is an array of responses sampled at a series of depths, usually separated by 100 μm. The 'z-axis' is the line along which a depth profile is sampled (e.g. Fig. 2). There was conduction of impulses along the

z-axis from the site of stimulation towards the pia, independent of synaptic transmission. We refer to this path of 'direct' conduction as 'on-beam'. The rest of the cortex was 'off-beam'. A 'horizontal profile' is an array of responses sampled moving from on-beam to off-beam while remaining at the same depth and following the plane of the slice. The 'y-axis' is the axis along which we made an electrode penetration, crossing perpendicular to the plane of the slice.

After each recording, the location was confirmed with Nissl-stained sections from the slices (cf. Fig. 1 in ref. 40). The white matter lay 1,350–1,400 μm from the pial surface in both living slices and the Nissl sections; shrinkage of slices during fixation was therefore insignificant. Because the boundary between layers II and III was indistinct, it is useful to refer to these collectively as layer II/III. However, we refer to the region of layer II/III bordering layer I as 'layer II', and the region bordering layer IV as 'layer III'. Stimulation was applied to the border of the white matter and layer VI in the manner previously described[40]. Usually, a single stimulation was applied once every 4 s; otherwise, paired stimuli were applied, 20 ms apart, with pairs 4 s apart (eg. Fig. 1).

In experiments in which the horizontal spread of excitation was studied, we sectioned the white matter with iridectomy scissors 0.5 mm medial and lateral to the site of stimulation. Field potentials were recorded with broken-tipped glass micropipettes filled with 2 M NaCl (DC impedances of 5–25 MΩ). All data were recorded near midway between the rostral and caudal cut faces (100–300 μm into the slice with respect to the y-axis). All field potential data are averages of 15–25 consecutive trials.

Single unit activity was recorded extracellularly to observe firing patterns of neurons not injured by impalements. Single unit potentials were distinguishable as such because they were sensitive to minor alterations in the recording position, were all-or-none with respect to strength of stimulus, and exhibited 'jitter' (variable latency). When the intent was to record single unit activity, we used unbroken glass micropipette electrodes (25–45 MΩ), made finer advances along the y-axis, and examined unaveraged responses. In some cases (eg. Fig. 5), we recorded field potentials with these same electrodes. The same filter settings were used for recording single units and field potentials (bandpass from 0.1 Hz to 3 kHz).

To better resolve the relationship of transmembrane current flow to cortical laminae, we have calculated profiles of second derivatives with respect to the z-axis, using the sampling interval as our 'differentiating grid'. Provided that certain simplifying assumptions are valid, this amounts to a 'one-dimensional current source–density (CSD) analysis'[22,46,53]. We discuss elsewhere the validity of these assumptions for the rat visual cortex slice preparation[40].

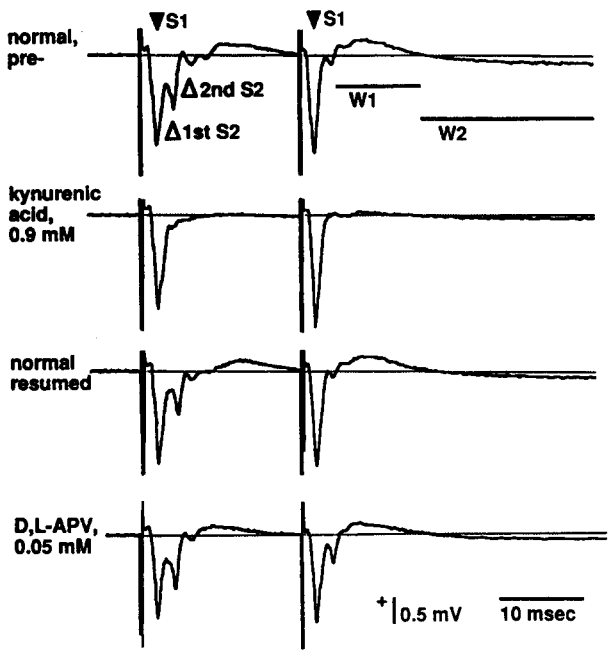

Fig. 1. Near elimination of components S2, W1 and W2 by kynurenic acid, and the lack of this effect by APV. Field potentials were recorded in layer III, on-beam, during an 85 min interval, without electrode repositioning. In this experiment, paired stimuli (20 ms apart) were delivered once every 4 s; the traces shown are averages of 15–25 consecutive responses. In drug-free (normal) medium, the response includes an S1 spike (▼), three S2 spikes (△), and the two slower waveforms, W1 and W2. Component W1 consists principally of a dipole (and sink–source pair) distributed across layers I and II (cf. ref. 40 and Fig. 2 of this paper). However, it is sometimes accompanied by a small positive potential in layer III, following the S2 spikes and preceeding component W2. In contrast with component W1, W2 exhibits maximal negativity in layer III. This figure includes only its rising phase. Medium containing kynurenic acid was added 16 min before the second trace, and discontinued 23 min before the third. Following washout of kynurenic acid, application of D,L-APV did not block any of these components, but altered appreciably the time–course of component W1.

RESULTS

Cortical field potentials following single shocks to the white matter were composed of the 4 components that we have described previously and named S1, S2, W1, and W2 (Figs. 1 and 2). These are identified by their latencies, durations, and whether or not they depend upon synaptic transmission. The magnitude and polarity of each component varies in a characteristic manner with respect to position along the radial axis (i.e. position with respect to cortical lamination), and each component's magnitude and latency varies in a characteristic manner with respect to horizontal (tangential) displacement from the radial axis of stimulation. Component S1 (spike S1) occurs on-beam only, between 2.5 and 5 ms latency, whereas the first S2 spike occurs between 5.5 and 7.5 ms after stimulation, and later S2 spikes recur at intervals of 3–4 ms for a total burst duration of roughly 15 ms. S1 and S2 spikes are followed by the slower components, W1 and W2, which are radially oriented field potential (and current source/sink) dipoles. (For a more detailed description and interpretation of these, refer to ref. 40 and the discussion section of this report.)

Components S1, S2, and W2 all have their greatest magnitudes in layer III, where they occur sequentially and distinct from each other. To make quantitative assessment of chosen drug concentrations, we left the recording electrode at a single location in layer III while changing bath solutions (e.g. Fig. 1). This was done to avoid effects of differences in electrode position between samplings. However, we also compared depth profiles (which required repositioning of the electrode) recorded in the presence and absence of pharmacological agents (e.g. Fig. 2); these depth profiles facilitated qualitative judgements about drug effects throughout the cortex from the pial surface down to the superficial half of layer V.

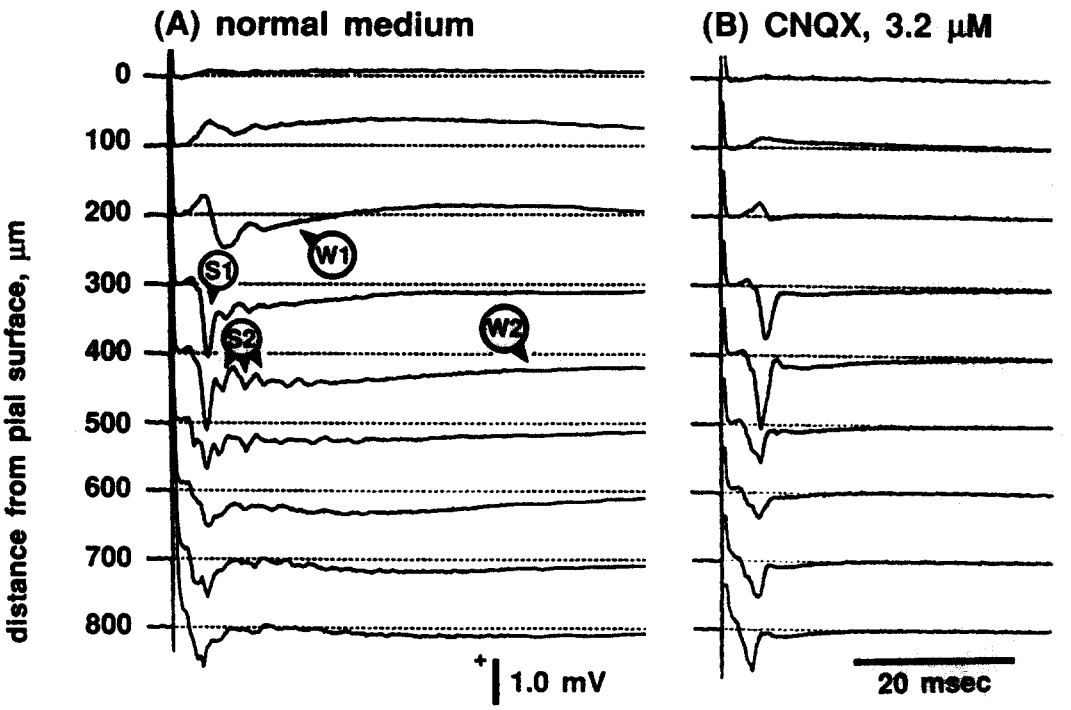

Fig. 2. Depth profiles recorded on-beam (A) in normal medium, and then (B) along the same radial axis in the same medium with 3.2 μM CNQX. The pointers with circled labels S1, S2, W1, and W2 indicate the 4 field potential components described in the text. After recording the profile in B, resumption of normal medium brought the return of S2 spikes recorded at 400 μm depth (not shown).

Effects of AMPA / kainate receptor blockade

We first examined the effects of kynurenic acid because it blocks both the NMDA and AMPA/kainate subtypes of glutamate receptor (reviewed in ref. 10).

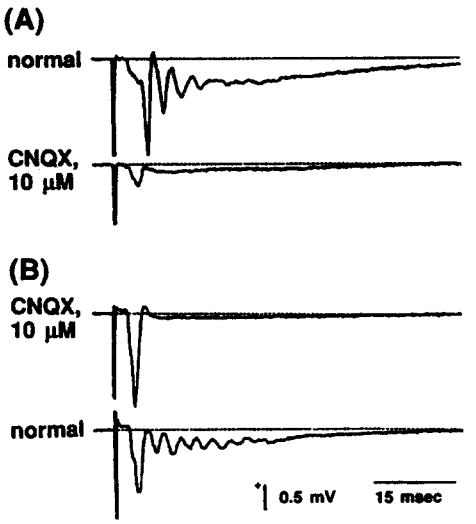

Fig. 3. Block of S2 spikes by CNQX (A) off-beam and (B) on-beam. All data were recorded in layer III, 350 μm from the pial surface. The upper trace in A was recorded in drug-free medium, and the lower trace from the same location after 20 min in medium containing CNQX. The small, early spike that remains in CNQX medium is the S1 component. The traces in B were recorded where the S1 spike was maximal, based on a horizontal profile (not shown here; cf. ref. 40) recorded after sampling the data in A, while continuing with medium containing CNQX. The horizontal profile indicated that the data in A were recorded 350 μm medial to the beam center. The lower trace in B was recorded after returning to drug-free medium.

Recording from layer III, on-beam and off-beam, we assessed the actions of kynurenic acid (0.5–1.0 mM) in 4 slices. S1 spikes were not inhibited at either concentration. However, S2 spikes and components W1 and W2 were nearly eliminated at 0.9 mM (Fig. 1). At 0.5 mM, S2 spikes and components W1 and W2 were completely suppressed off-beam but were only partially blocked on-beam (not shown). The effects of kynurenic acid were reversible.

CNQX is a glutamate receptor antagonist which blocks AMPA/kainate receptors at low micromolar concentrations[17,32]. We collected on-beam depth profiles before and during application of medium with 3.2

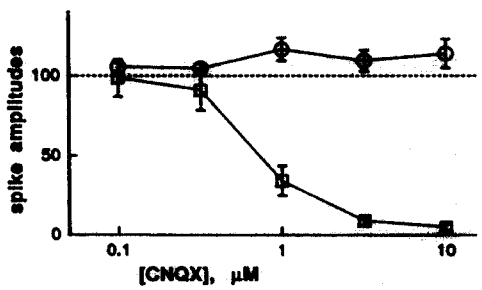

Fig. 4. Amplitudes of population spikes in layer III as a function of the concentration of CNQX applied via the bath. (□) Mean amplitudes of the first S2 spike (which occurs between 5 and 9 ms after stimulation). (○) Mean amplitudes of S1 spikes. Data were pooled from 8 experiments, with each data point normalized with respect to the response amplitude in normal medium at that same recording site. Overall, the mean S2 spike amplitude in normal medium was 0.76 mV (1 S.E.M. = 0.19); the normal mean S1 amplitude was 1.00 mV (1 S.E.M. = 0.18). Each error bar represents 1 S.E.M.

μM CNQX (Fig. 2). In normal medium, the responses included the 4 identified components. Application of CNQX resulted in a complete block of components S2, W1 and W2; there were no spike-like waveforms after 5 ms latency, no negative potential at 200 μm depth between 5 and 15 ms, and after 40 ms there was no potential greater than 0.05 mV, regardless of depth (Fig. 2B). As with slices treated with kynurenic acid or low Ca^{2+} medium[40], the S1 spike was not inhibited by CNQX.

In medium containing CNQX, the S1 spike is followed by a low amplitude dipole, negative at 300–500 μm depth and positive at 100 μm. There also occurs a small and brief negative potential between 600 and 800 μm depth. Thus, CNQX treatment differs from treatment with Ca^{2+}-free medium in that Ca^{2+}-free medium eliminates all appreciable field potentials beyond 5 or 6 ms[40]. The persistence of late, slow potentials during CNQX treatment is probably due, at least in part, to currents gated by NMDA receptors (see below).

Responses off-beam were also sensitive to CNQX. The uppermost trace in Fig. 3A is typical of a response in layer III displaced 350 μm from the central axis of the column stimulated. The prominent burst of S2 spikes began 6.5 ms after stimulation and the S1 spike was nearly absent. Application of 10 μM CNQX sup-

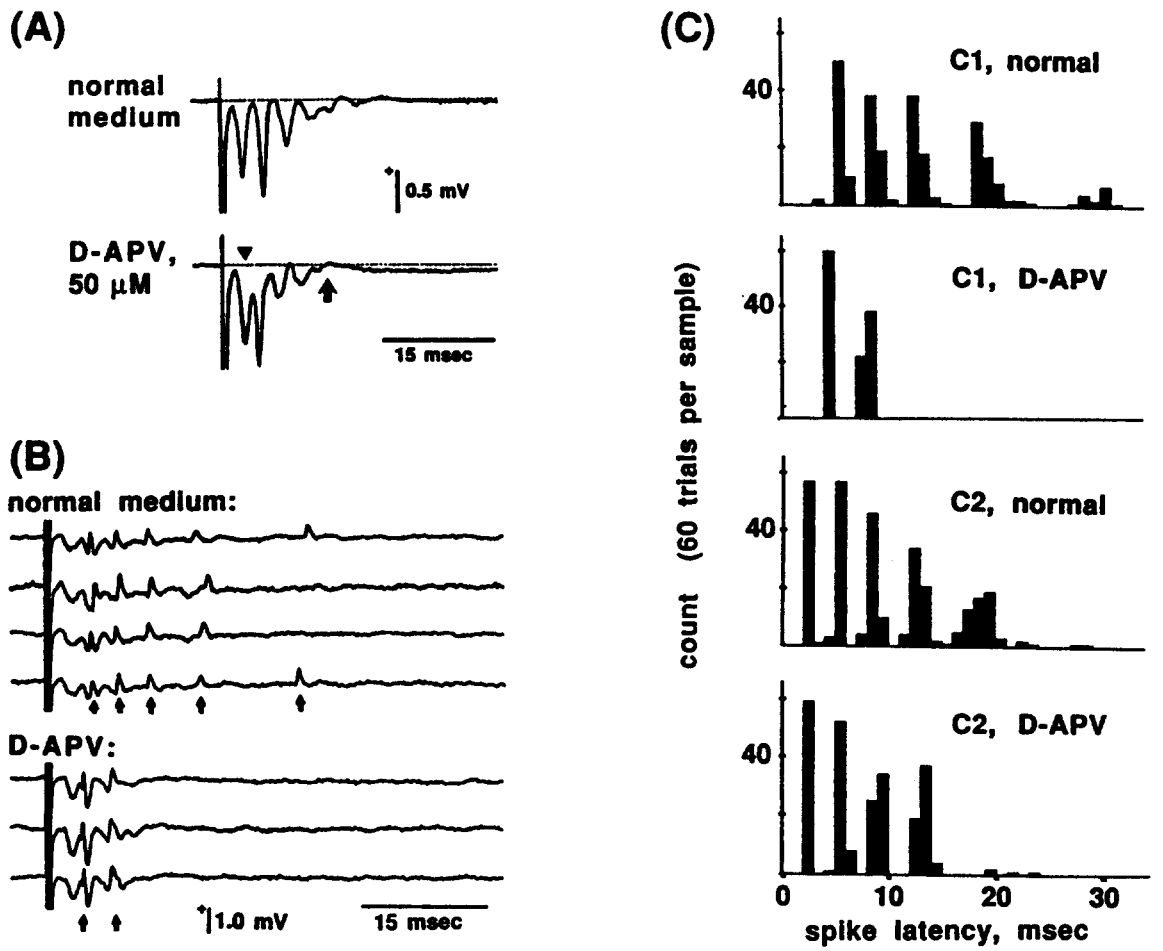

Fig. 5. Effects of APV on (A) population spike bursts and (B and C) single unit activity in layer III. In A, the response includes a S1 spike (▼) and a burst of rapidly decaying S2 spikes. Application of APV did not prevent S2 spike bursts, but shortened their duration to 12 ms (arrow). The peak (and the decay) of the W2 component occurs earlier during APV treatment; measured 90 ms post-stimulation (not shown), this potential was −0.068 and −0.029 mV in normal and APV-treated slices, respectively. These data were recorded 47 min apart without intervening movement of the electrode. The normal response was recorded after the response in D-APV, 34 min after changing to medium without drug. B: the effect of treatment with D-APV on the firing bursts of a single unit in the same slice. (The field potentials in part A were recorded from this same location in the slice, after losing contact with this unit.) Unlike the potentials that we present in all other figures, these are individual trials, not averages. For the bottom trace in each group, examples of unitary potentials are indicated by arrows. The first downward inflection is the S1 field potential spike, unaccompanied by a single-unit spike. The first single unit spike is superimposed upon the S2 field potential spike. In D-APV, its falling phase appears larger because it occurs slightly earlier and is thereby superimposed upon the negative-going phase of the S2 spike. C: histograms summarizing 60 responses of this same cell (C1) and a second cell (C2) in this same slice preparation. In normal medium, the mean response of cell C1 was 4.25 spikes per stimulation (1 S.D. = 0.47). In D-APV, every stimulation evoked precisely 2 spikes in cell C1; these occurred roughly 1 ms earlier than their corresponding spikes in normal medium. Cell C2 fired in synchrony with both S1 and S2 field potential spikes. D-APV had little or no effect on firings synchronized with the S1 and first three S2 spikes, but almost completely prevented later firing. In normal medium, stimulation evoked a mean of 5.00 spikes (1 S.D. = 0.26) in cell C2. In D-APV, the mean response was 4.07 spikes (1 S.D. = 0.25).

pressed this burst and unmasked the small S1 spike that precedes it with a latency-to-peak of 4.6 ms (Fig. 3A, lower trace). Remaining in layer III, we recorded a horizontal profile (not shown) and found that component S1 was largest 350 μm lateral to the initial location. There, it was 1.8 mV in magnitude (Fig. 3B, upper trace), with a latency of 4.1 ms.

CNQX effects as a function of concentration

At sufficiently high concentrations, CNQX antagonizes the function of both NMDA and AMPA/kainate receptors[17,26,32]. We assessed the relationship between concentration of CNQX and the block of S2 spikes to determine whether these were due to a selective block of AMPA/kainate receptors. CNQX at 0.1 μM had no significant effect on S2 spike amplitudes, but inhibited these almost completely at 10 μM (Fig. 4). The level of inhibition varied in a concentration-dependent manner at 3 intermediate concentrations. Interpolating, there was 50% inhibition at roughly 0.7 μM. Block by CNQX at such low concentrations is not likely to be due to effects on NMDA receptors (see Discussion).

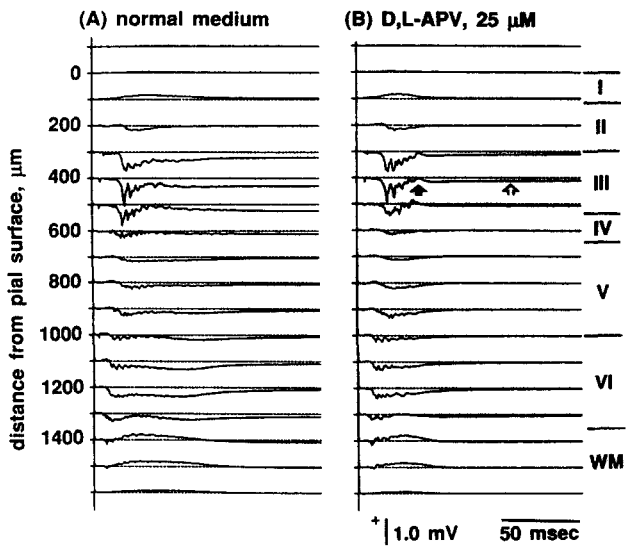

Fig. 6. Depth profiles depicting the effect of APV on field potentials recorded far off-beam, 1.5 mm medial to the beam center. Each trace is an average of 20 trials. (Positions of the cortical laminae are identified at the far right. However, the border between layers II and III was chosen somewhat arbitrarily.) In this slice, burst firing in layer III spread horizontally for 1.8 mm. The off-beam response included a burst of S2 spikes and a long, W2-like negative potential in layer III. However, component S1 was absent and W1 was very small or absent. The off-beam spike bursts recorded at this location invariably began 17 ms after stimulation (whereas the latency of on-beam spike bursts ranged from 2.5 to 4.5 ms). As with S2 spikes on-beam, APV reduced the duration of off-beam S2 spike bursts, but did not prevent them. In medium with APV, rapid inflections ceased completely 20 ms after bursts began (filled arrow). APV also reduced the amplitude of the slow, W2-like potential which followed each burst (open arrow). The off-beam response in drug-free medium also included rapid, low-amplitude inflections and slow potentials in layers V and VI. Application of APV did not effect these rapid inflections, but accelerated the decay of these slow potentials.

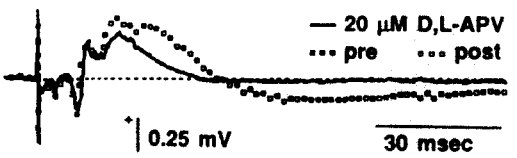

Fig. 7. Effects of APV on slow waveforms recorded in layer III, 650 μm medial to the beam center. In this preparation there were relatively large slow potentials beginning 25 ms after stimulation and lasting for roughly 125 ms. This is an extreme case in which the W2 component was completely blocked by APV. These averaged responses in APV were recorded after 10 min of application; the post-treatment responses were recorded after 7 min of drug-free medium.

Application of CNQX often increased the amplitude of S1 spikes (Figs. 3 and 4), as did other treatments that inhibited glutamatergic transmission (kynurenic acid, Fig. 1, and APV, Fig. 11). This effect may have been due to elimination, in antidromically actived cells, of shunting and de-synchronizing effects of synaptically induced currents.

NMDA receptors and coherent firing by layer III neurons

The above data indicate that S2 spikes are generated via a mechanism involving activation of AMPA/kainate receptors. We examined whether or not generation of S2 spikes also depends on the activation of NMDA receptors by assessing the effect of applying APV, a specific antagonist NMDA receptors. In spinal cord and hippocampus, 50 μM D,L-APV produces a selective and virtually complete block of responses evoked either synaptically or by challenges with NMDA[14,27]. Our analysis is based on experiments in which 20–75 μM D,L-APV was applied in otherwise normal medium ($n = 7$), and later experiments in which 0.1, 0.32, 1.0, 3.2, 10 and 50 μM D-APV (the active stereoisomer) were applied in normal medium ($n = 8$), medium lacking Mg^{2+} ($n = 5$), normal medium with CNQX ($n = 2$), and in Mg^{2+}-free medium with CNQX ($n = 4$).

Block of NMDA receptors never prevented S2 bursts, whether observed on-beam (Figs. 1 and 5A) or off-beam (Fig. 6). However, APV consistently reduced the duration of bursts lasting longer than 15 ms. Typically, an S2 burst ends with several low amplitude inflections that continue for 20 ms or more after the initial spike, (e.g. Figs. 1, 3, 5A, and 6A). APV eliminated these late inflections. In APV, each burst ended definitively, between 12 and 20 ms after the initial spike (solid arrows in Figs. 5A and 6). In normal medium (i.e. containing 1.2 mM Mg^{2+}), APV had no appreciable effect on the duration of bursts that ended in less than 12 ms (Fig. 7).

When electrodes suitable for recording single-unit activity were advanced into layer III, units that fired in

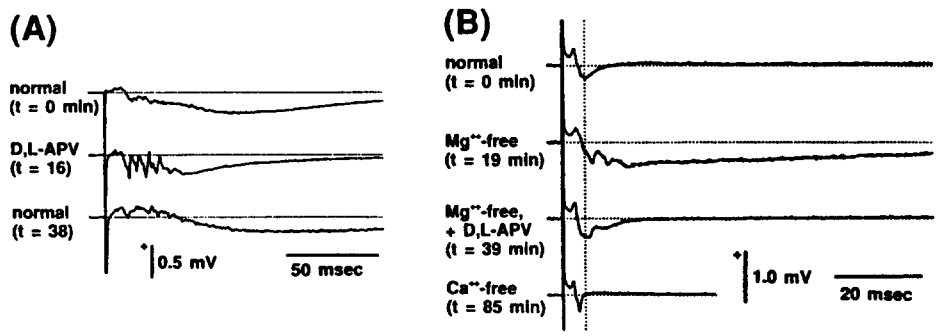

Fig. 8. A: field potentials and a superimposed single unit in layer III, 0.8 mm lateral to the beam center; averages of 20 trials. D,L-APV (40 μM) was introduced at t = 3 min; washout began at t = 18 min. B: unmasking of NMDA receptor activation by application of Mg^{2+}-free medium. This treatment results in long, slow negative potentials, beginning first in layer II, then in layer III. These responses were recorded in layer II, 100 μm from the pial surface; hence, S2 spikes are absent. The effect of Mg^{2+}-free medium is almost completly reversed by application of APV. Finally, application of Ca^{2+}-free medium reveals the purely antidromic response. The vertical dotted line demarcates a latency of 5.5 ms, after which all potentials depend upon synaptic function. Each trace is an average of 15 or more trials. All data were recorded without intervening movement of the recording electrode.

phase with population spikes S1 and S2 were readily encountered (Fig. 5B; see also ref. 40). The bursts fired by such units were affected by APV application in a manner consistent with effects of the drug on S2 population spikes. We recorded one such unit from the same location as the field potentials in Fig. 5A. It fired a mean of 4.25 times per stimulation in normal medium (1 S.D. = 0.47), with its earliest spikes coinciding closely with the 3 largest S2 spikes (Fig. 5B,C). Such latencies imply that all of this unit's firings were synaptically driven; this was confirmed when application of CNQX silenced this unit (not shown). In 50 μM D-APV, this unit fired only twice with each stimulation, once between 4 and 5 ms, and once between 7 and 9 ms.

In the same slice, after resuming normal medium, a different unit fired a mean of 5.00 times per stimulation (1 S.D. = 0.26), with the first 4 unit spikes closely coinciding with the S1 and S2 spikes in the field potential (Fig. 5A,C). After applying D-APV a second time, however, this unit fired a mean of only 4.07 spikes per burst (1 S.D. = 0.25). APV application had essentially the same effect on this single unit's burst duration as it did on the duration of S2 population spike bursts.

These and previously reported field potential and single unit data[40,41] indicate that firing was highly coherent for the first 4 volleys of each burst, and sporadic thereafter. Late out-of-phase activity could be responsible for the late, low-amplitude inflections that follow bursts of S2 spikes in field potential recordings. APV selectively inhibited this late, out-of-phase firing. In addition to merely suppressing out-of-phase firing, however, application of APV actually enhanced phase-locked firing of some units. Fig. 8A presents an example of unitary activity superimposed on a field potential recorded 0.8 mm off-beam in layer III. Each trace is an

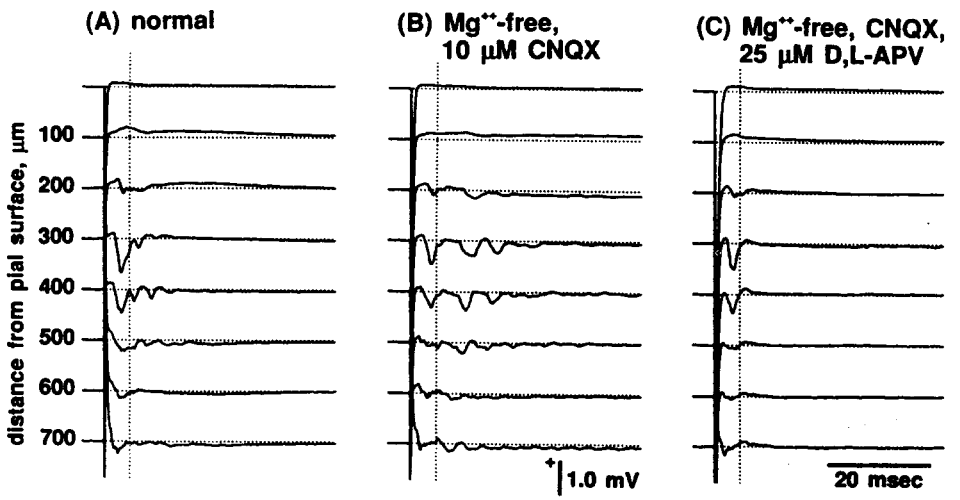

Fig. 9. On-beam depth profiles illustrating APV-sensitive field potentials in CNQX-containing medium that is Mg^{2+} free. A: in normal medium, this preparation exhibited typical S1 and S2 components. (Components W1 and W2 were small and are not apparent at this scale.) B: in medium contain 10 μM CNQX but not Mg^{2+}, there occurred rapid deflections with a spatial profile characteristic of S2 spikes, but which recurred at one half the usual frequency for S2 spike bursts. C: these were eliminated by addition of APV to the medium.

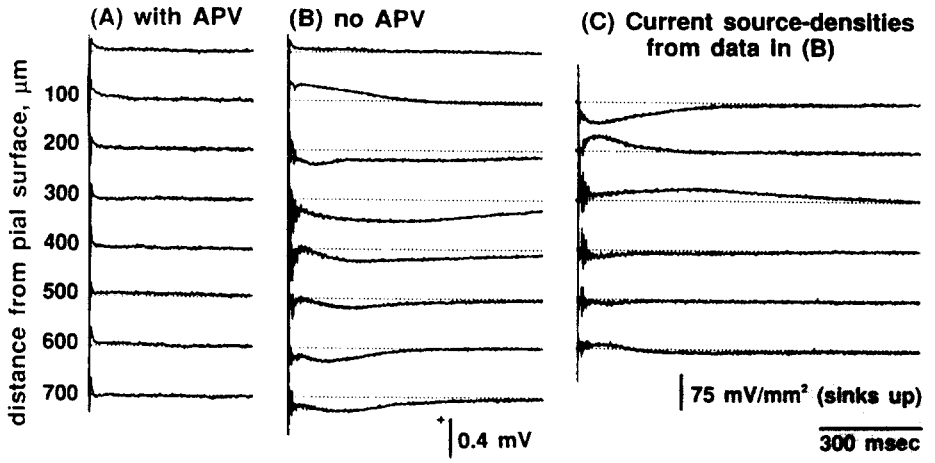

Fig. 10. On-beam depth profiles and current source-density analysis of APV-sensitive slow potentials present in medium containing CNQX (10 μM) without Mg^{2+}. These data were recorded from the same slice and along the same radial track as the data in Fig. 9, but with a 15-fold longer time base. A: in the presence of 25 μM D,L-APV, all slow waves are eliminated. B: the profile of field potentials recorded in medium without APV. C: current source-densities derived from the data in B. During the first 150 ms, there is a high sink density in layer II (depth = 200 μm), coinciding with a source in layer I. As this dipole decays, sink density increases at 300 μm depth. In their depth distributions, these two components resemble that of components W1 and W2 in normal medium (cf. ref. 40) except that they rise and decay much more slowly.

average of 20 trials; sporadically occurring spikes are therefore not represented, whereas unitary firing of unvarying latency appears as a sharp inflection superimposed upon slower field potential waveforms. In normal medium (top trace), no coherent firing is evident. In the presence of APV, the unit fired a burst of 4 spikes with unvarying latency. The unitary firing pattern closely resembled that expected for an S2 population spike burst at this distance off-beam[40]: it began after a latency of 11 ms and contained 4 spikes separated initially by 4.5 ms. Once returned to drug-free medium, this unit no longer fired coherently.

Enhancement of firing coherency during APV treatment is also evident from the latency histograms of cell 'C1' presented in Fig. 5C. In the absence of APV, the first and second S2 spikes of cell C1 occur in any of 5 histogram latency bins (each 1 ms wide). During application of D-APV, latencies of the first and second S2 spikes fall exclusively within 3 bins.

In 3 preparations, application of APV resulted in some shortening of the latency of S2 spikes. This is exemplified in Fig. 5C, in which those unitary S2 spikes of cell C1 that remained during treatment with APV occurred 1 to 2 ms earlier. The drug application had a similar effect on S2 population spikes recorded from this same preparation (Fig. 5A).

APV and responses of long latency and duration

In normal medium, S2 spikes were followed by the slower field potentials W1 and W2 (Figs. 1, 2A, 6A, and 7). Application of APV primarily affected the later portions of these slow potentials, resulting in decreased latency-to-peak, faster decay and smaller peak amplitudes. The greatest effect of APV occured in preparations in which these components were especially long-lasting (Figs. 6B and 7); more often, APV had only a minor effect on the duration of slow waves (Fig. 1).

Except when post-synaptic membranes are depolarized, channels gated by NMDA receptors are blocked by Mg^{2+} at concentrations present both physiologically and in our normal medium[34,49,55]. Since our single-shock stimulations were likely to produce only transient post-synaptic depolarizations, we expected that NMDA receptors could only make a limited contribution to responses in normal medium. We therefore examined effects of APV in Mg^{2+}-free medium. In every case, Mg^{2+}-free medium greatly prolonged slow potentials. Subsequent application of APV almost entirely reversed this effect of Mg^{2+}-free medium (Fig. 8B).

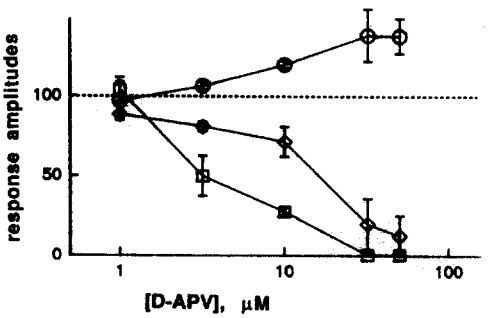

Fig. 11. Percent inhibition of APV-sensitive field potentials as a function of the [D-APV] applied via the bath. All responses were recorded in medium containing CNQX but no Mg^{2+}. (○) Mean amplitudes of S1 spikes. (□) Mean amplitudes of the first S2-like spike (cf. Fig. 9B). (◇) Mean amplitudes of the slow W2-like potential (measured at 30 ms latency, cf. Fig. 10B). The data are from 3 preparations, with each data point normalized with respect to the response amplitude in normal medium at the same recording site. The mean amplitudes for S1 spikes, S2-like spikes, and W2-like potentials were 0.84, 0.32, and 0.29 mV, respectively. The error bars represent 1 S.E.M.

We examined the effects of APV in slices treated with CNQX in Mg^{2+}-free medium ($n = 4$) to observe currents gated by NMDA receptors in isolation from contributions of AMPA/kainate receptors. Because the kinetics of NMDA receptor-gated channels are inherently slow[5,34,44,50], we were surprised to find that S2-like spikes occurred in such slices (Fig. 9), particularly since CNQX abolishes S2 spikes in normal medium (Figs. 2 and 3). Like S2 spikes in normal medium, these were prominent in layer III only. Distinct from normal S2 spikes, these recurred at about one half the normal frequency. These spikes were always less than 0.5 mV in amplitude. Responses in Mg^{2+}-free medium with CNQX also included slow dipoles which exhibited the same sink–source distributions as components W1 and W2 in normal medium, but with much slower rise and fall (Fig. 10; see also ref. 40).

These S2-like spikes with a 7 ms periodicity and the slow dipoles with depth distributions like components W1 and W2 were all eliminated by treatment with APV in a concentration-dependent manner (Fig. 11). However, the slow S2-like spikes were more sensitive to APV than were the W1- and W2-like dipoles. The amplitude of the slow S2 spikes was reduced by half when the [D-APV] was about 3 μM, a value similar to that obtained with D-APV in a study of antagonism of NMDA receptors in the hippocampus[27]. In contrast, 50% inhibition of the slow W2-like potential required a roughly 4-fold higher [D-APV].

DISCUSSION

We have used selective glutamate receptor antagonists to assess the respective roles of AMPA/kainate and NMDA receptors in the generation of field potentials in visual neocortex. Because field potentials are infrequently used in studies of neocortical neurotransmission, this discussion begins with a rationale for their use, and a brief review of how we interpret neocortical field potentials evoked in normal, drug-free medium.

Primarily based on data from outside of the neocortex, there are 2 commonly recognized kinds of field potential that can be synaptically driven: (1) 'field EPSPs', the relatively slow extracellular potentials generated by subthreshold excitatory postsynaptic currents, and (2) 'population spikes', brief extracellular potentials generated by neurons firing in synchrony near the recording site. Because population spikes are generated by summation of rapid and brief unitary currents, they tend to be highly localized and their amplitudes highly dependent on synchrony of unitary contributions[52]. This makes them especially useful for locating concentrations of synchronously active neurons. Because field potential data represent the average activity of populations of neurons, they are more readily reproducible than single-unit data. Because they are routinely stable over periods of many hours, field potential recordings are well suited for studies which examine concentration vs. inhibition relationships (eg. ref. 37 and present data) or effects of pathway use on synaptic efficacy (eg. refs. 1,8,35,43).

Previous investigators have discussed in detail methods used to localize membrane currents that generate field potentials[45,52,53]. Based on these methods, in our previous[40] and present studies, we have recorded and analyzed spatial distributions (depth profiles) of neocortical field potentials to arrive at the working hypothesis, corroborated by single-unit data, that field potential components, S1 and S2, are population spikes generated by synchronously firing neurons in lamina III. Similarly, we attribute components W1 and W2 to radially oriented currents which presumably flow in the apical dendrites of pyramidal cells.

We discuss elsewhere the many factors likely to be responsible for differences in field potential profiles from one study to the next[40]. Previously published accounts of field potentials in the neocortex in vitro have included waveforms resembling S1 and S2 spikes[1,35,43,62], but generally waveforms have comprised either the S1 spike alone, a single S2 component alone, or repeating S2 spikes of low amplitude. We treat S2 spikes as a discrete component, whereas previous investigators have not. To encourage convergent 'network' activity, we have used relatively thick slices (500 μm), fully submerged, with upper and lower faces exposed to rapidly moving medium; we apply stronger stimulations than are used in intracellular recordings of subthreshold postsynaptic potentials, and we precisely position the recording site with respect to the region of layer III that is antidromically activated.

Field potentials that resemble S2 spikes are also evoked in vivo by electrical stimulation of the optic tract, lateral geniculate nucleus, or the optic radiation[7,47]. However, we know of no reports of S2-like potentials evoked by visual stimulation, and, electrical shock being a highly non-physiological form of stimulation, we do not propose that such a high level of firing coherence occurs during visual function. We study field potentials S2, W1 and W2 because the synaptic transmission that generates them may participate in normal neocortical function and in pathological states such as epilepsy; these experiments are not an attempt to mimic or simulate the complexity of visual function in the slice.

Some may regard S2 spikes as a form of epileptiform activity, in that similar waveforms are induced in

hippocampal slices by disinhibitory agents used to model epilepsy[61], and the presently observed shortening of neocortical S2 spike bursts by APV appears similar to the effect of APV on repetitive field potential spikes in hippocampus[15]. Hypothetically, epileptiform activity could be produced in the absence of GABA receptor antagonists if GABAergic neurons were especially vulnerable to the trauma of slice preparation. However, coherent firing phase-locked to the stimulus is not a prominent feature of activity in neocortex treated with GABA receptor antagonists, as we have discussed elsewhere[40]. Such treatments produce paroxysmal, all-or-none field potentials that, after an abrupt beginning, are very long lasting[6,11]. Unlike S2 spikes, these paroxysmal potentials are widespread throughout the middle cortical laminae. However, S2 spikes are graded as a function of stimulus strength, and occur with a constant and brief latency, besides also being brief in duration and confined to layer III. Differing from epileptiform firing, the generation of S2 spikes requires that neurons fire in phase with each other, and not that they merely be synchronously active. Some of our slices exhibited conventional epileptiform activity (as defined in ref. 6) in the absence of any GABA receptor antagonist. However, such responses tended to be unstable and these slices were not included in the present study. In some slices, S2 spikes were very low in amplitude, or absent. When such slices were treated with bicuculline, the result was not enhancement of S2 spikes, but rather typical epileptiform potentials (Langdon and Sur, unpublished). A final consideration is that disinhibition, should it occur, would not in itself interfere with the study of excitatory neurotransmission. Indeed, it is conventional to block GABAergic transmission when the goal is to observe excitatory neurotransmission at certain synapses, such as mossy fiber inputs to pyramidal cells in the CA3 subfield of hippocampus[3,70].

Antagonist concentrations versus level of block

An essential assumption underlying our differentiation of roles of receptor subtypes is that the observed effects of antagonists were caused by specific actions of CNQX and APV on the AMPA/kainate and NMDA subtypes of glutamate receptor, respectively. Because there is only a narrow range of concentrations within which CNQX blocks AMPA/kainate receptors without inhibiting NMDA receptor function (see below), we chose methods that maximized control over the drug concentrations to which receptors were exposed. Slices were studied in a submersion-type chamber and antagonists were applied via the bath medium. Regardless of concentration, onsets of drug effect were completed within 20 min, whereas the field potential components that we studied were stable for hours. Thus it was practical to allow extracellular concentrations within the slices to equilibrate with bath concentrations, presumably leading to well-defined and spatially uniform drug concentrations within slices.

Data from other brain slice preparations and from neuronal cell cultures indicate that block of AMPA/kainate receptors is considerable if the [CNQX] exceeds 0.5–1.0 μM, whereas interference with NMDA receptor function is small or negligable unless the [CNQX] is greater than 5 μM[17,23,69]. In a study of antagonism of effects of iontophorectically applied agonists on layer III pyramidal cells (in rat frontal cortex), responses to quisqualate were greatly reduced by 5 μM CNQX, whereas higher concentrations of CNQX were needed to block responses to NMDA[23]. In our study, 1.0 μM CNQX reduced amplitudes of S2 population spikes by 70%, and 3.3 μM CNQX reduced these to less than 10% of their normal amplitude. These concentrations should have had little effect on NMDA receptors. Moreover, only those S2 spikes with the longest latencies were sensitive to concentrations of D-APV expected to eliminate neurotransmission mediated by NMDA receptors. Thus we conclude that the S2 population spikes depend, at least for their initiation, upon synaptic transmission mediated by AMPA/kainate receptors.

Concerning actions of APV, these were almost certainly due to block of NMDA receptors; D-APV has an apparent K_D for the NMDA receptor of about 2 μM, and does not interfere with function of AMPA/kainate receptors (or any other known neurotransmitter) unless the concentration exceeds at least 50 μM[10]. Spike-like waveforms (elicited in Mg^{2+}-free medium) were sensitive to lower concentrations of APV than were late, slow waves (Fig. 11), but the amplitudes of both were reduced by at least 85% in 50 μM D-APV.

What synapses drive S2 spikes?

Because of the complexity and divergent nature of neocortical connections, it is generally not possible to attribute with certainty an electrophysiological response to the action of a specific, anatomically defined class of synapse. Concerning the present data, it is known that white matter stimulation produces direct activation of layer III pyramidal cells (as evidenced by the S1 spike), and these neurons project locally, onto each other. A simple explanation for S2 spikes is therefore that they are driven by this local network of recurrent projections[40]. For the present, we use this explanation as a working hypothesis, without excluding,

however, the possibility that other inputs to layer III cells are partly or even wholly responsible for S2 spikes.

There are a number of published studies of the effects of glutamatergic antagonists on neocortical synapses (among others, refs. 1, 2, 30, 35, 54, 63, 65–67). Because experiments differed with respect to cortical area, lamina, species, response component latencies, and stimulus position and strength, no two studies appear to overlap entirely. For example, our study shares in common with the work of Nishigori, Kimura and collaborators a focus upon responses of rat visual cortex layer III neurons to white matter stimulation. However, the previous experiments were primarily concerned with responses to input from fast-conducting afferents ascending from the white matter, whereas the present experiments were primarily concerned with relatively long latency, responses in layer III following antidromic activation via slowly (~ 0.3 m/s) conducting efferents to the white matter. Thus, synaptically driven (CNQX-sensitive) spikes occur in this previous study with the same latency (2–4 ms) as our non-synaptically elicited S1 spikes, and our earliest synaptically driven spike (the first S2 spike) occurs 3 ms after the beginning of apparent poly-synaptic activity in their study. We conclude that we have examined a later and different event in the chain of responses to white matter stimulation.

The time-course of AMPA / kainate and NMDA receptor-mediated responses

A common theme in all the data is that the extent to which a response component depended upon inputs meditated by either AMPA/kainate or NMDA receptors was largely a function of latency. Present and previous data show that roughly 6 ms must pass before current gated by NMDA receptors makes an appreciable contribution to responses to single-shock stimulations. The strength of this contribution then augments during the subsequent 10 ms or longer. The data are consistent with a hypothesis that the presence of NMDA receptors is pervasive in supragranular circuitry, with intrinsic properties of this ligand-gated ion channel being an essential determinant of its role in evoked response.

This importance of latency is consistent with known differences in the inherent kinetics of ion gating by AMPA/kainate and NMDA receptors. In hippocampus, EPSPs and excitatory post-synaptic currents (EPSCs) mediated by AMPA/kainate receptors typically rise in less than 3 ms and fall rapidly thereafter[8,9,29,42,70]. Similar data have come from spinal cord[33], optic tectum[37], as well as elsewhere in the brain (reviewed in refs. 10 and 31). In contrast, postsynaptic currents gated by NMDA receptors rise slowly, over 10–20 ms, and decay even more slowly[9,18,29,44].

Components S2, W1 and W2 almost certainly result via activation of a mixture of mono- and polysynaptic pathways. Each synchronous compound spike in a coherent burst could be driven by synchronized convergence of excitatory inputs onto layer III neurons, especially if these superimposed upon depolarizing afterpotentials (arising intrinsically). The most effective EPSCs to drive these coherent bursts would have both rapid onset and short duration, as does the EPSC mediated by AMPA/kainate receptors. In contrast, the current gated by NMDA receptors would be better suited to determine the duration of firing bursts and influence the number of neurons joining in coherent firing, without providing sufficient input to drive individual action potentials.

Extracellular [Mg^{2+}], membrane potential and NMDA receptors

A second distinction between AMPA/kainate and NMDA receptors is that the flow of ion current gated by the NMDA receptor channel is blocked to varying extents by physiological levels of Mg^{2+}, with the level of block depending upon the post-synaptic membrane potential. As a consequence, a combination of agonist with this receptor may lead to a state of "occult conductance"[5]: after transmitter has bound to the receptor, depolarization arising via activation of nearby AMPA/kainate (or perhaps other) receptors will reveal and be augmented by the otherwise latent contribution of the NMDA receptor channels. After a single activation, the state of occult conductance may last for several tens of milliseconds.

Although there was a variable and usually minor effect of APV on responses in normal medium, this NMDA receptor antagonist greatly inhibited responses evoked in bath media that lacked Mg^{2+}. In such media, APV-sensitive response components began with latencies as short as 6 ms (Fig. 8). Removal of Mg^{2+} is expected to have many effects in addition to disinhibition of currents gated by NMDA receptors[65]. However, it is reasonable to interpret effects of APV on responses in this medium as due to block of NMDA receptors. It is clear from our data that these receptors are present in sufficient numbers as to be able to greatly influence neocortical excitability. This was most evident when responses were studied in Mg^{2+}-free medium that also contained sufficient CNQX to block most post-synaptic current gated by AMPA/kainate receptors. A surprising result was that slices so treated retained the ability to generate population spikes in layer III, although these recurred at about one half the

frequency of 'normal' S2 spikes (and were lower in amplitude). Clearly, these slower spikes were driven by activity of NMDA receptors, in that they were reduced to 30% of normal amplitude by 10 μM D-APV, and eliminated by about 30 μM. Removal of Mg^{2+} from the medium presumably reveals the occult conductance of activated NMDA receptor otherwise undetected. Our data indicate that the full contribution of NMDA receptors to cortical responses can occur rapidly and be substantial, provided that Mg^{2+} block of the channel is removed.

Implications concerning visually evoked responses

Responses to visual input may be determined, in part, by selective activation of cooperative neuronal groups, with local excitatory interactions between lamina III cells playing a significant role in defining these groups and the forms of input to which they respond[40]. By this hypothesis, glutamate antagonists applied in vivo would alter visually evoked responses indirectly, by inhibiting local excitatory interactions (in addition to direct effects on thalamocortical transmission). The present data indicate that the most rapid local excitatory interactions are driven by AMPA/kainate receptors. However, activation of NMDA receptors could contribute significantly to local excitatory interactions during slower or more sustained visual responses, depending on the ability of summation and convergence to overcome Mg^{2+}-mediated channel block. Studied in vivo, the visually evoked responses of cells in the superficial layers of visual cortex of adult cat are more sensitive to block of NMDA receptors[19,24,51] than the responses to single shocks that we have studied in vitro. This difference may reflect a greater ability of visually driven inputs (arriving as streams of thalamofugal spikes) to override the Mg^{2+} block of NMDA receptor channels, thus revealing their occult conductance. The role of NMDA receptors in the visual neocortex may be analogous to those in the lateral geniculate nucleus; there, the responses of a cell to sustained visual stimulation often depends heavily on NMDA receptors[28,36,64]. In the thalamus in vitro, the major effect of block of the NMDA receptor is on the later portions of EPSPs evoked by single shocks applied to the optic nerve[16]. Similarly, activation of NMDA receptors in visual neocortex may depend significantly on the temporal summation of sustained inputs from the LGN, as well 'background' excitatory inputs, including those not originating from within the visual system.

Our data have two additional implications concerning NMDA receptors and visually driven responses: (1) the inhibition of visually driven responses in layer III by applications of APV may be due partly to reductions in the duration of firing bursts in individual cells; (2) changes in the level of input mediated by NMDA receptors may alter the extent to which layer III neurons fire in or out of phase with one another. By such a mechanism, drug applications could alter subtle aspects of visual function without necessarily changing the number of spikes elicited by each presentation of a stimulus pattern.

ABBREVIATIONS

AMPA	α-amino-3-hydroxy-5-methyl-4-isoxazole propionic acid
APV	2-amino-5-phosphonovalerate
CNQX	6-cyano-7-nitroquinoxaline-2,3-dione
CSD	current source–density
EPSC	excitatory post-synaptic current
EPSP	excitatory post-synaptic potential
LGN	lateral geniculate nucleus

Acknowledgements. We are grateful to Manny Esguerra, Duncan Kuhn, and Terry Sullivan for their valuable contributions, both intellectual and technical. This research was supported NIH Grant EY-07023.

REFERENCES

1 Aroniadou, V.A. and Teyler, T.J., The role of NMDA receptors in long-term potentiation (LTP) and depression (LTD) in rat visual cortex, *Brain Res.*, 562 (1991) 136–143.
2 Artola, A. and Singer, W., The involvement of *N*-methyl-D-aspartate receptors in induction and maintenance of long-term potentiation in rat visual cortex, *Eur. J. Neurosci.*, 2 (1990) 254–269.
3 Barrionuevo, G., Kelso, S.R., Johnston, D. and Brown, T.H., Conductance mechanism responsible for long-term potentiation in monosynaptic and isolated excitatory synaptic inputs to hippocampus, *J. Neurophysiol.*, 55 (1986) 540–550.
4 Bear, M.F., Kleinschmidt, A., Gu, Q. and Singer, W., Disruption of experience-dependent synaptic modifications in striate cortex by infusion of an NMDA receptor antagonist, *J. Neurosci.*, 10 (1990) 909–925.
5 Bekkers, J.M. and Stevens, C.F., Computational implications of NMDA receptor channels, *Cold Springs Harbor Symp. Quant. Biol.* 55 (1990) 135.
6 Chagnac-Amatai, Y. and Connors, B.W., Horizontal spread of synchronized activity in neocortex and its control by GABA-mediated inhibition, *J. Neurophysiol.*, 61 (1989) 747–758.
7 Chang, H.-T. and Kaada, B., An analysis of primary response of visual cortex to optic nerve stimulation in cats, *J. Neurophysiol.*, 13 (1950) 305–318.
8 Collingridge, G.L., Kehl, S.J. and McLennan, H., Excitatory amino acids in synaptic transmission in the Schaffer collateral–commissural pathway of the rat hippocampus, *J. Physiol.*, 334 (1983) 33–46.
9 Collingridge, G.L., Herron, C.E. and Lester, R.A.J., Synaptic activation of *N*-methyl-D-aspartate receptors in the Schaffer collateral–commissural pathway of rat hippocampus, *J. Physiol.*, 399 (1988) 283–300.
10 Collingridge, G.L. and Lester, R.A.J., Excitatory amino acid receptors in the vertebrate central nervous system, *Pharmacol. Rev.*, 40 (1989) 143–207.
11 Connors, B.W., Initiation of synchronized neuronal bursting in neocortex, *Nature*, 310 (1984) 685–687.
12 Constantine-Paton, M., Cline, H.T. and Debski, E., Patterned activity, synaptic convergence, and the NMDA receptor in developing visual pathways, *Annu Rev. Neurosci.*, 13 (1990) 129–154.

13 Davies, S.N. and Lodge, D., Evidence for involvement of *N*-methylaspartate receptors in 'wind-up' of class 2 neurones in the dorsal horn of the rat, *Brain Res.*, 424 (1987) 402–406.

14 Davies, J., Francis, A.A., Jones, A.W. and Watkins, J.C., 2-Amino-5-phosphonovalerate (2APV), a potent and selective antagonist of amino acid-induced and synaptic excitation, *Neurosci. Lett.*, 21 (1981) 77–81.

15 Dingledine, R., Hynes, M.A. and King, G.L., Involvement of *N*-methyl-D-aspartate receptors in epileptiform bursting in the rat hippocampal slice, *J. Physiol.*, 380 (1986) 175–189.

16 Esguerra, M., Kwon, Y.H. and Sur, M., Retinogeniculate EPSPs recorded intracellularly in the ferret lateral geniculate nucleus in vitro: role of NMDA receptors, *Vis. Neurosci.*, *Vis. Neurosci.*, 8 (1992) 545–555.

17 Fletcher, E.J., Martin, D., Aram, J.A., Lodge, D. and Honoré, T., Quinoxalinediones selectively block quisqualate and kainate receptors and synaptic events in rat neocortex and hippocampus and frog spinal cord in vitro, *Br. J. Pharmacol.*, 95 (1988) 585–597.

18 Forsythe, I.D. and Westbrook, G.L., Slow excitatory post-synaptic currents mediated by *N*-methyl-D-aspartate receptors on cultured mouse central neurones, *J. Physiol.*, 396 (1988) 515–533.

19 Fox, K., Sato, H. and Daw, N., The location and function of NMDA receptors in cat and kitten visual cortex, *J. Neurosci.*, 9 (1989) 2443–2454.

20 Gean, P.-W. and Chang, F.-C., Ketamine suppresses synchronized discharges in the disinhibited amygdala slice, *Brain Res. Bull.*, 26 (1991) 923–927.

21 Gilbert, C.D. and Wiesel, T.N., Laminar specialization and intracortical connections in the cat primary visual cortex. In F.O. Schmidt, F.G. Worden, G. Adelman, and S.G. Dennis (Eds.), *The Organization of the Cerebral Cortex*, MIT Press, Cambridge, MA, 1981, pp. 163–191.

22 Haberly, L.B. and Shepherd, G.M., Current–density analysis of summed evoked potentials in opossum prepyriform cortex, *J. Neurophysiol.*, 36 (1973) 789–802.

23 Hablitz, J.J. and Sutor, B., Excitatory post-synaptic potentials in rat neocortical neurons in vitro. III. Effects of a quinoxalinedione non-NMDA receptor antagonist, *J. Neurophysiol.*, 64 (1990) 1282–1290.

24 Hagihara, K., Tsumoto, T., Sato, H. and Hata, Y. Actions of excitatory amino acid antagonists on geniculo-cortical transmission in the cat's visual cortex, *Exp. Brain Res.*, 69 (1988) 407–416.

25 Hahm, J., Langdon, R.B. and Sur, M., Disruption of retinogeniculate afferent segregation by antagonists to NMDA receptors, *Nature*, 351 (1991) 568–570.

26 Harris, K.M. and Miller, R.J., CNQX (6-cyano-7-nitroquinoxaline-2,3-dione) antagonizes NMDA-evoked [^{3}H]GABA release from cultured cortical neurons via an inhibitory action at the strychnine-insensitive glycine site, *Brain Res.*, 489 (1989) 185–189.

27 Harris, E.W., Ganong, A.H. and Cotman, C.W., Long-term potentiation in the hippocampus involves activation of *N*-methyl-D-aspartate receptors, *Brain Res.*, 323 (1984) 132–137.

28 Heggelund, P. and Hartveit, E., Neurotransmitter receptors mediating excitatory input to cells in the cat lateral geniculate nucleus. I. Lagged cells, *J. Neurophysiol.*, 63 (1990) 1347–1360.

29 Hestrin, S., Sah, P. and Nicoll, R.A., Mechanisms generating the time–course of dual component excitatory synaptic currents recorded in hippocampal slices, *Neuron*, 5 (1990) 247–253.

30 Hirsch, J.A. and Gilbert, C.D., Synaptic physiology of horizontal connections in the cat's visual cortex, *J. Neurosci.*, 11 (1989) 1800–1809.

31 Holmes, W.R. and Levy, W.B., Insights into associative long-term potentiation form computational models of NMDA receptor-mediated calcium influx and intracellular calcium concentration changes, *J. Neurophysiol.*, 63 (1990) 1148–1168.

32 Honoré, T., Quinoxalinediones: potent competitive non-NMDA glutamate receptor antagonists, *Nature*, 241 (1988) 701–703.

33 Jahr, C.E. and Yoshioka, K., Ia afferent excitation of motoneurones in the in vitro new-born rat spinal cord is selectively antagonized by kynurenate, *J. Physiol.*, 370 (1986) 515–530.

34 Jahr, C.E. and Stevens, C.F., A quantitative description of NMDA receptor-channel kinetic behavior, *J. Neurosci.*, 10 (1990) 1830–1837.

35 Kimura, F., Nishigori, A., Shirokawa, T. and Tsumoto, T. Long-term potentiation and *N*-methyl-D-aspartate receptors in the visual cortex of young rats, *J. Physiol.*, 414 (1989) 125–114.

36 Kwon, Y.H., Esguerra, M. and Sur, M., NMDA and non-NMDA receptors mediate visual responses of neurons inthe cat's lateral geniculate nucleus, *J. Neurophysiol.*, 66 (1991) 414–428.

37 Langdon, R.B. and Freeman, J.A., Antagonists of glutaminergic neurotransmission block retinotectal neurotransmission in goldfish, *Brain Res.*, 398 (1986) 169–174.

38 Langdon, R.B., Esguerra, M. and Sur, M., Transmission events in mammalian visual cortex that involve NMDA and non-NMDA glutamate receptors, *Soc. Neurosci. Abstr.*, 14 (1988) 200.

39 Langdon, R.B., Kuhn, D.M. and Sur, M., Synchronous, coherent burst-firing by neurons in lamina III of rat visual cortex in vitro, *Soc. Neurosci. Abstr.*, 15 (1989) 797.

40 Langdon, R.B. and Sur, M., Components of field potentials evoked by white matter stimulation in isolated slices of primary visual cortex: spatial distributions and synaptic order, *J. Neurophysiol.*, 64 (1990) 1484–1501.

41 Langdon, R.B. and Sur, M., Single-unit activity corresponding to population bursts in layer III of rat primary visual cortex in vitro, *Soc. Neurosci. Abstr.*, 16 (1990) 1218.

42 Langdon, R.B., Johnson, J.W. and Barrionuevo, G., Time–course and plasticity of rat hippocampal CA3 pyramidal cell responses to input from recurrent collaterals examined by whole-cell recordings, *Soc. Neurosci. Abstr.*, 17 (1991) 1330.

43 Lee, K.S., Sustained enhancement of evoked potentials following brief, high-frequency stimulation of the cerebral cortex in vitro, *Brain Res.*, 239 (1982) 617–623.

44 Lester, R.A.J., Clements, J.D., Westbrook, G.L. and Jahr C.E., Channel kinetics determine the time–course of NMDA receptor-mediated synaptic currents, *Nature*, 346 (1990) 565–567.

45 Llinás, R. and Nicholson, C., Analysis of field potentials in the central nervous system. In C.F. Stevens (Ed.), *Handbook of Electroencephalography and Clinical Neurophysiology, Vol. 2B*, Elsevier, Amsterdam, 1974, pp. 61–83.

46 Lorente de Nó, R., Action potential of the motoneurons of the hypoglossus nucleus, *J. Cell. Comp. Physiol.*, 29 (1947) 207–287.

47 Malis, L.I. and Kruger, L., Multiple response and excitability of cat's visual cortex, *J. Neurophysiol.*, 19 (1956) 172–186.

48 Martin, D. and Lodge, D., Ketamine acts as a non-competitive *N*-methyl-D-aspartate antagonist on frog spinal cord in vitro. *Neuropharmacology*, 24 (1985) 999–1003.

49 Mayer, M.L., Westbrook, G.L. and Guthrie, P.B., Voltage-dependent block by Mg^{2+} of NMDA responses in spinal cord neurones, *Nature*, 309 (1984) 261–263.

50 Mayer, M.L. and Westbrook, G.L., The action of *N*-methyl-D-aspartic acid on mouse spinal neurones in culture, *J. Physiol.*, 361 (1985) 65–90.

51 Miller, K.D., Chapman, B. and Stryker, M.P., Visual responses in adult cat visual cortex depend on *N*-methyl-D-aspartate receptors, *Proc. Natl. Acad. Sci. USA*, 86 (1989) 5183–7187.

52 Mitzdorf, U., Current source-density method and application in cat cerebral cortex: investigation of evoked potentials and EEG phenomena, *Physiol. Rev.*, 65 (1985) 37–100.

53 Nicholson, C. and Freeman, J.A., Theory of current source–density analysis and determination of conductivity tensor for anuran cerebellum, *J. Neurophysiol.*, 38 (1975) 356–368.

54 Nishigori, A., Tsumoto, T. and Kimura, F., Contribution of quisqualate/kainate and NMDA receptors to excitatory synaptic transmission in the rat's visual cortex, *Vis. Neurosci.*, 5 (1990) 591–604.

55 Nowak, L., Bregestovski, P., Ascher, P., Herbet, A. and Prochiantz, A., Magnesium gates glutamate-activated channels in mouse central neurones, *Nature*, 307 (1984) 462–465.

56 Parnavelas, J.G., Lieberman, A.R. and Webster, K.E., Organization of neurons in the visual cortex, area 17, of the rat, *J. Anat.*, 124 (1977) 305–322.

57 Paxinos, G. and Watson, C., *The Rat Brain in Stereotaxic Coordinates*, 2nd edn., Academic Press, New York, 1986.

58 Peters, A. and Kara, D.A., The neuronal composition of area 17 of rat visual cortex. I. The pyramidal cells, *J. Comp. Neurol.*, 234 (1985) 218–241.

59 Rothman, S.M., Thurston, J.H., Hauhart, R.E., Clark, G.D., and Solomon, J.S., Ketamine protects hippocampal neurons from anoxia in vitro, *Neuroscience*, 21 (1987) 673–378.
60 Salt, T.E., Excitatory amino acid receptors and synaptic transmission in the rat ventrobasal thalamus, *J. Physiol.*, 391 (1987) 499–510.
61 Schwartzkroin, P.A. and Prince, D.A., Cellular and field potential properties of epiliptogenic hippocampal slices, *Brain Res.*, 147 (1978) 117–128.
62 Shaw, C. and Teyler, T.J., The neural circuitry of the neocortex examined in the in vitro brain slice preparation, *Brain Res.*, 243 (1982) 35–47.
63 Shirokawa, T., Nishigori, A., Kimura, F. and Tsumoto, T., Actions of excitatory amino acid antagonists on synaptic potentials of layer II/III neurons of the cat's cortex, *Exp. Brain Res.*, 78 (1989) 489–500.
64 Sillito, A.M., Murphy, P.C., Salt, T.E. and Moody, C.I., Dependence of retinogeniculate transmission in cat on NMDA receptors, *J. Neurophysiol.*, 63 (1990) 347–355.
65 Sutor, B. and Hablitz, J.J., EPSPs in rat neocortical neurons in vitro. II. Involvement of *N*-methyl-D-aspartate receptors in the generation of EPSPs, *J. Neurophysiol.*, 61 (1989) 621–634.
66 Thomson, A.M., A magnesium-sensitive post-synaptic potential in rat cerebral cortex resembles neuronal responses to *N*-methylaspartate, *J. Physiol.*, 370 (1986) 531–549.
67 Thomson, A.M. and West, D.C., *N*-Methylaspartate receptors mediate epileptiform activity evoked in some, but not all conditions in rat neocortical slices, *Neuroscience*, 19 (1986) 1161–1177.
68 Tsumoto, T., Masui, H. and Sato, H., Excitatory amino acid transmitters in neuronal circuits of the cat visual cortex, *J. Neurophysiol.*, 55 (1986) 469–483.
69 Verdoorn, T.A., Kleckner, N.W. and Dingledine, R. *N*-methyl-D-aspartate/glycine and quisqualate/kainate receptors expressed in *Xenopus* oocytes: antagonist pharmacology, *Mol. Pharmacol.*, 35 (1989) 360–368.
70 Williams, S.H. and Johnston, D., Kinetic properties of two anatomically distinct excitatory synapses in hippocampal CA3 pyramidal neurons, *J. Neurophysiol.*, 66 (1991) 1010–1020.
71 Zilles, K., Wree, A., Schleicher, A. and Divac, I., The monocular and binocular subfields of the rat's primary visual cortex: a quantitative approach, *J. Comp. Neurol.*, 226 (1984) 391–402.
72 Zilles, K., *The Cortex of the Rat: A Stereotaxic Atlas*, Springer-Verlag, Berlin, 1985.